ELSEVIER

Journal of Power Sources 84 (1999) 225–230

JOURNAL OF POWER SOURCES

www.elsevier.com/locate/jpowsour

The effect of metal oxides as co-catalysts for the electro-oxidation of methanol on platinum–ruthenium

K. Lasch *, L. Jörissen, J. Garche

Center for Solar Energy and Hydrogen Research Baden-Wuerttemberg, Division 3, Electrochemical Energy Storage and Conversion, Helmholtzstr. 8, Ulm D-89081, Germany

Accepted 28 June 1999

Abstract

The electrocatalytic activities of different ternary platinum–ruthenium (Pt–Ru)–metal-oxides have been investigated in half cell experiments, by cyclic voltammetry and stationary current–voltage measurements. The results are compared to binary Pt–Ru alloy catalysts. The materials have been prepared using a modification of the Adams method. X-ray analytical methods (X-ray diffraction, XRD; energy dispersive X-ray spectroscopy, EDX; X-ray photoelectron spectroscopy, XPS) have been used to characterize the composition, particle size and crystallinity of the catalysts, and their surface areas have been determined by the Brunauer–Emmet–Teller (BET) method. The catalyst materials consist of varying amounts of metal oxides and Pt–Ru alloy particles. BET surface areas of 80–120 m^2/g have been measured corresponding to particle diameters of the order of 3–5 nm. The results of electrochemical measurements demonstrate that introduction of a transition metal oxide (WO_x, MoO_x, VO_x) leads to an improvement of the catalytic activity towards methanol oxidation.

Keywords: Electro-oxidation; Methanol; Pt–Ru alloys; Ternary compounds; Transition metal oxides

1. Introduction

One of the main problems of the direct methanol fuel cell (DMFC) is the still insufficient activities of the anode catalysts [1]. Pure platinum is poisoned by reaction intermediates such as CO_{ads} [2,3]. In order to improve the catalyst performance, platinum alloys (typically platinum–ruthenium, Pt–Ru) are used in DMFCs. Platinum accomplishes the dissociative chemisorption of methanol, whereas ruthenium forms a surface oxy-hydroxide which subsequently oxidizes the carbonaceous adsorbate to CO_2 [4,5].

A large number of investigations have been reported on the use of platinum and platinum alloys supported on metal oxides [6,7] and metal sulfides [8] in order to enhance the electro-oxidation of methanol. However, Pt–Ru alloys remain the most active catalysts for this purpose.

In a different approach recently reported by Götz and Wendt [9,10], an increased catalytic activity has been found when ternary catalysts based on a Pt–Ru system were used.

In this work, the electro-oxidation of methanol on ternary Pt–Ru–metal-oxide catalysts is reported.

2. Experimental

2.1. Catalyst preparation and characterization

The catalysts were prepared using a modification of the method of Adams and Schriner [11]. Appropriate amounts of the noble metal halides and transition metal oxides were intimately mixed with an excess of sodium nitrate and the mixture was heated to 500°C for 3 h. The solidified melt was then washed thoroughly with water to remove nitrate and chloride, and the resulting aqueous suspension of mixed oxides was reduced at room temperature with bubbling hydrogen [12].

The bulk composition of the catalyst materials was investigated by EDX. An attempt was made to determine the surface composition of the catalyst powders by X-ray photoelectron spectroscopy (XPS). The spectra were back-

* Corresponding author.
E-mail: kerstin.lasch@huba.zsw.uni-ulm.de;
Internet: http:// www.zsw.uni-ulm.de

0378-7753/99/$ - see front matter
PII: S0378-7753(99)00321-3

Table 1
Properties of catalyst materials

Catalyst	Bulk composition (EDX) [at.%]	Surface composition (XPS) [at.%]	BET surface area [m^2/g]
Pt–Ru	55% Pt; 45% Ru	64% Pt; 36% Ru	82
Pt–Ru–WO_x; Pt:W = 8:1	54% Pt; 39% Ru; 7% W	49% Pt; 44% Ru; 7% W	120
Pt–Ru–MoO_x; Pt:Mo = 7:1	56% Pt; 36% Ru; 8% Mo	38% Pt; 51% Ru; 11% Mo	108
Pt–Ru–VO_x; Pt:V = 7:1	52% Pt; 40% Ru; 8% V	58% Pt; 42% Ru; V not determined	90

ground-corrected using the Shirley [13] method and Gaussian–Lorentz routines were used to fit the resulting peaks. The quantitative evaluation of each species was carried out by dividing the integrated peak area by empirical atomic sensitivity factors [14].

The geometric surface areas of the catalyst were determined by the BET method using nitrogen as the adsorbate.

Particle size and crystallinity of the materials were investigated by XRD. Spectral contributions of the copper $K_{\alpha 2}$ line were subtracted by a Rachinger algorithm correction. To assess the particle size, the Pt(220) peak was fitted to a Gaussian lineshape using a linear baseline correction.

2.2. Electrochemical measurements

The preparation of the thin film electrodes followed the method recently described by Schmidt et al. [15]. Glassy carbon electrodes (12 mm diameter, 1.131 cm^2) served as substrate for the catalyst materials. Catalysts were dispersed ultrasonically in water in a concentration of 2 mg/ml and a 160-μl aliquot was transferred onto a glassy carbon substrate, yielding a catalyst loading of 280 $\mu g/cm^2$. After evaporation of the water in a nitrogen stream, the resulting thin catalyst film was covered with 80 μl of a Nafion® solution in order to fix the particles on the substrate. The resulting Nafion® film had a thickness of about 0.2 μm. Therefore, it was sufficiently thin (< 0.5 μm) so that film diffusion effects were negligible under these conditions [16,17].

The catalysts were characterized at room temperature by cyclic voltammetry and stationary current–voltage curves in a three-electrode cell using a mercury–mercury-sulphate reference electrode. A solution of 1 M methanol in 0.5 M H_2SO_4 was used as the electrolyte. Potentials are referenced to the reversible hydrogen electrode (RHE).

3. Results and discussion

3.1. Catalyst composition

The results of EDX, XPS and BET surface area measurements are summarized in Table 1. The binding energy (BE) of the Ru $3d_{3/2}$ line in zerovalent ruthenium is 284.3 eV [18], which is very close to the C 1s line resulting from adsorbed carbonaceous species. Consequently, the Ru 3p spectra were also recorded and used for analysis. Vanadium could not be detected by XPS because the high-inten-

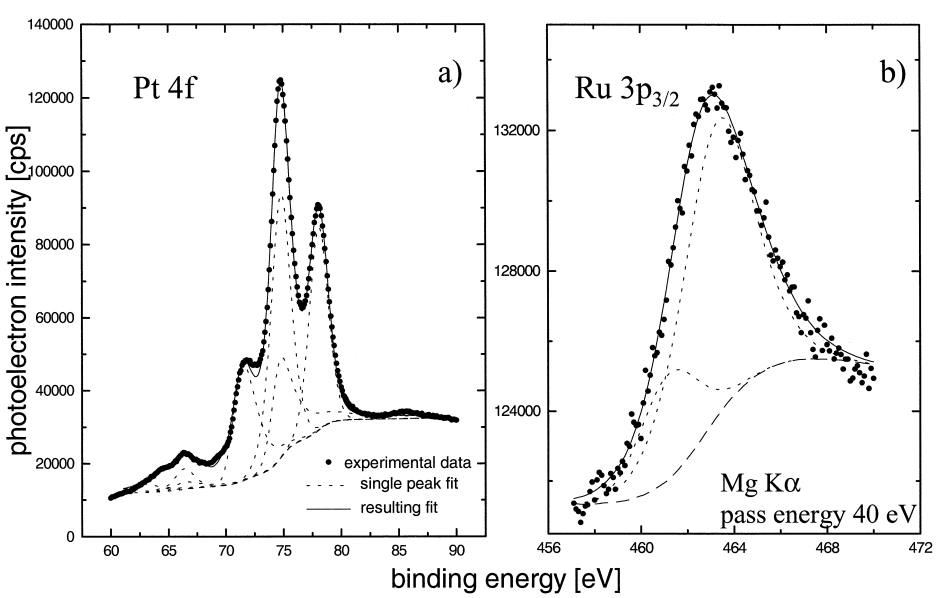

Fig. 1. Pt 4f and Ru $3p_{3/2}$ X-ray photoelectron spectra of a Pt–Ru catalyst.

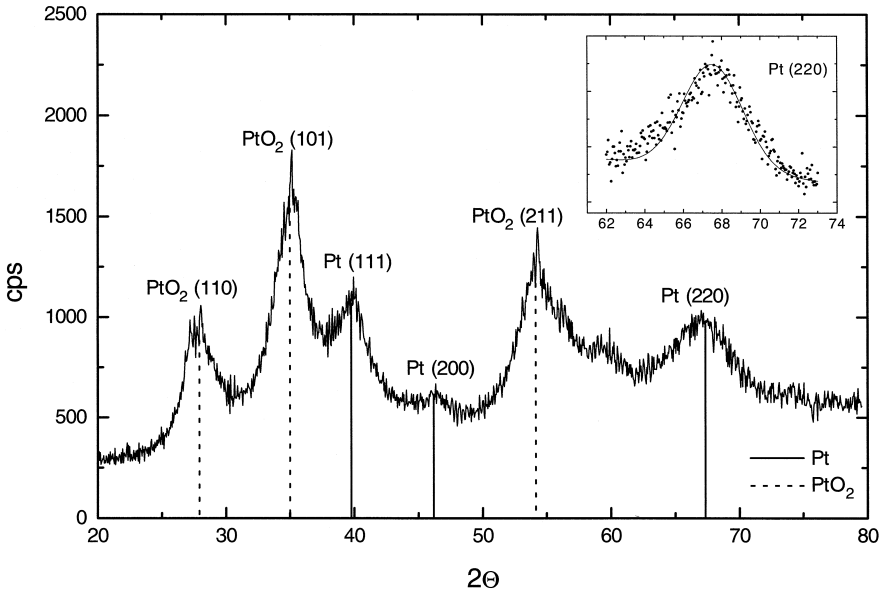

Fig. 2. XRD pattern of a ternary Pt–Ru–WO_x catalyst. Step size: 0.05°; step time: 45 s.

sity V 2p line was overlapping with the much stronger O 1s line. The lower-intensity V 2s line was too weak to be detected for analysis.

The quantitative EDX and XPS analysis shows that the bulk and surface composition of the materials are almost identical, taking into account the errors of both methods resulting from surface roughness.

The Pt 4f X-ray photoelectron spectrum of a Pt–Ru catalyst given in Fig. 1a suggests that the lower binding energy doublet with Pt $4f_{7/2}$ at 71.5 eV agrees well with the published values of Pt(0) while the BE of the Pt $4f_{7/2}$ component of the higher binding energy doublet at 74.7 eV is close to the chemical shift reported for Pt(IV) oxide [18]. The rather broad Ru $3p_{3/2}$ signal originates from (partially) oxidized Ru. The peaks at binding energies of 461.1 and 462.7 eV correspond to Ru(0) and RuO_2, respectively [19].

The results of XRD analysis indicate that the products contain varying amounts of noble metal oxides in addition to metal phases, which is in good agreement with the data obtained by XPS. The XRD pattern of a ternary catalyst (Pt–Ru–WO_x) is presented in Fig. 2. Apparently, XRD of the ternary catalysts failed to detect the presence of transition metal oxide peaks. As EDX- and XPS examinations of the ternary materials revealed the coexistence of platinum, ruthenium and transition metal oxides, these observations suggest that the transition metal oxides exist as an amorphous structure.

Furthermore, no diffraction peaks indicating the presence of a pure ruthenium phase appear. That means that either only ruthenium oxide phases, which are impossible to distinguish from the reflections of platinum oxides, are present or that ruthenium is alloyed with platinum. Considering the results from XPS analysis, where zerovalent ruthenium could be detected, it may be concluded that the catalysts are composed of Pt–Ru alloy particles next to Pt–Ru oxides and amorphous transition metal oxides.

3.2. Particle size and surface area

The BET surface areas ranging from 80 to 120 m^2/g correspond to particle sizes in the range 3–5 nm in diameter as calculated from a simple spherical particle model. The density of the $Pt_{50}Ru_{50}$ alloy was assumed to be 16.9

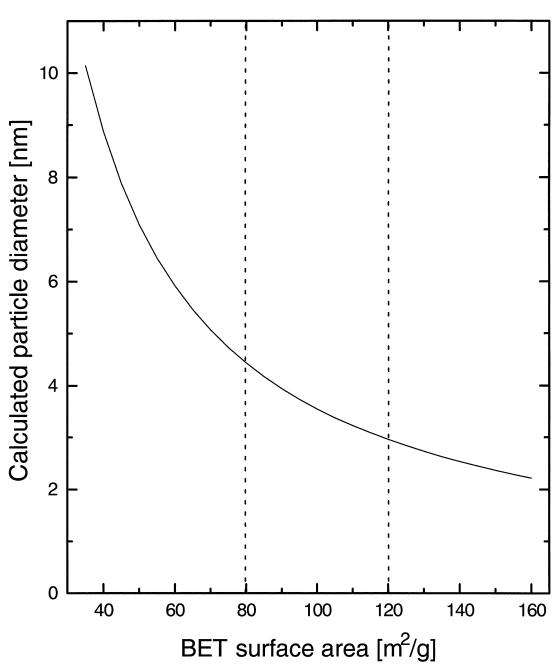

Fig. 3. Calculation of particle diameter from geometric surface area assuming a simple spherical model.

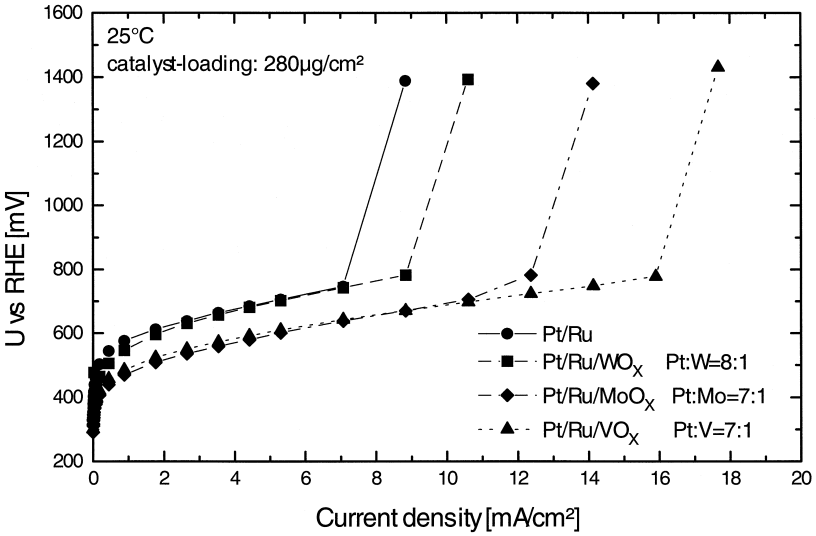

Fig. 4. Current–voltage characteristics of different catalysts.

g/cm^3. The calculated correlation of the surface area and the particle size is shown in Fig. 3.

An attempt has been made to estimate the particle size from the XRD data. However, the accuracy is limited since line broadening results not only from the small particle size, but also from overlapping peaks of different oxide phases.

The average particle size, L, was estimated from the Pt(220) diffraction peaks according to the Scherrer formula [20]:

$$L = \frac{0.9\lambda_{K\alpha_1}}{B_{2\Theta}\cos\Theta_{max}},$$

where $\lambda_{K\alpha 1}$ is the x-ray wavelength (1.54056 Å for Cu $K_{\alpha 1}$ radiation), $B_{2\Theta}$ is the width of the diffraction peak at half-height (in radians), and Θ_{max} is the angle at the position of the peak maximum. Hence, the calculation gives an average particle size of 3–5 nm. This result is in good agreement with the particle sizes calculated from BET surface areas (see Fig. 3). The absence of any sharp diffraction peaks indicates a unimodal particle distribution.

3.2.1. Electrochemical measurements

Fig. 4 shows stationary current–voltage characteristics of different catalysts (Pt–Ru plus transition metal oxides such as WO_x, MoO_x and VO_x).

In the metal oxide containing ternary catalysts, a lower polarization of the methanol oxidation has been observed. Furthermore, electrodes prepared from ternary catalysts are able to sustain higher current densities.

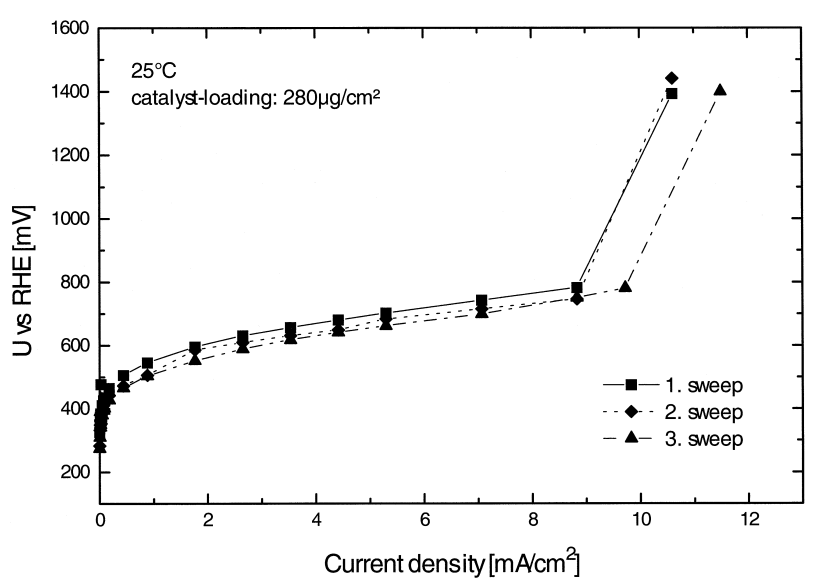

Fig. 5. Consecutive current–voltage curves of a Pt–Ru–WO_x electrode.

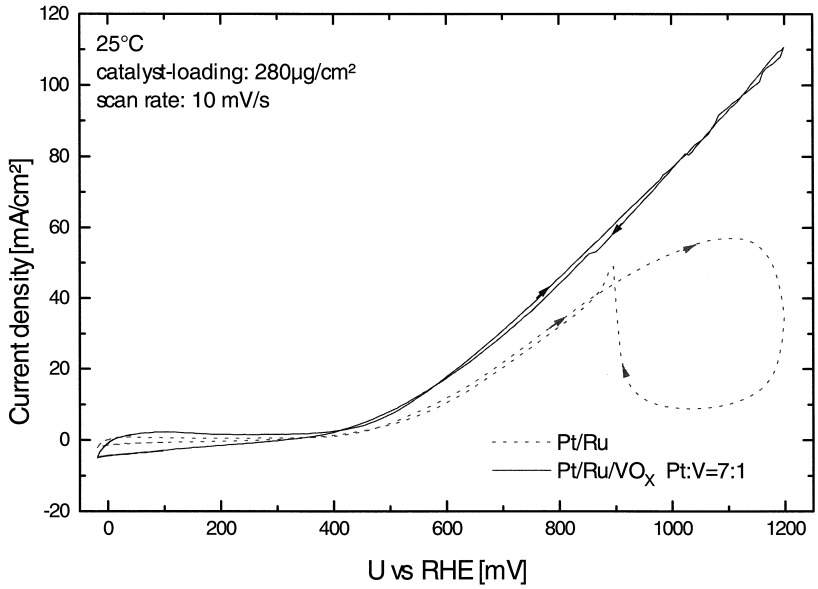

Fig. 6. Cyclic voltammetry of Pt–Ru and Pt–Ru–VO_x electrodes.

It is also evident that a severe deactivation of the catalyst materials occurs at potentials above 750 mV vs. RHE. This can be attributed to the formation of a catalytically inactive surface oxide. Consecutive current–voltage curves of a Pt–Ru–WO_x electrode are presented in Fig. 5. It can be shown that the formation of inactive surface species is reversible.

The deactivation of Pt–Ru is also visible in the cyclic voltammogram (Fig. 6). Fig. 7 shows the cyclic voltammogram of a ternary catalyst material (Pt–Ru–VO_x). It is evident that MeOH oxidation starts at a potential of 360 mV vs. RHE which is almost identical to the binary Pt–Ru electrode (380 mV). The most apparent difference of the cyclic voltammetry of the Pt–Ru–VO_x electrode is the increase in current density at potentials above 500 mV vs. RHE, and the fact that no deactivation can be observed at potentials below 1200 mV.

No catalyst corrosion effects are detected in the investigated potential range by voltammetry in pure H_2SO_4 (base voltammetry).

From these results, it can be concluded that the ternary compound slows down the process of surface oxide forma-

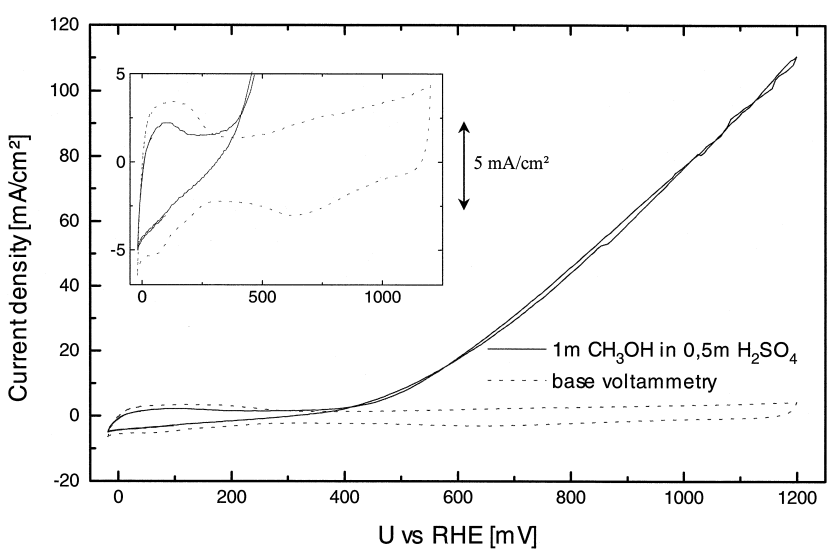

Fig. 7. Cyclic voltammetry of Pt–Ru–VO_x at 25°C, scan rate 10 mV/s.

tion. Furthermore, it can be assumed that the enhanced catalytic activity results from the redox processes of the transition metal oxides.

Such a mechanism has been reported earlier for tungsten oxides [21]. The co-catalytic activity is attributed to a rapid change of the oxidation state of W, involving the postulated redox couples W(VI)/W(IV) [22] or W(V)/W(VI) [23]. As Mo and V are known to form bronzes (similar to W), a similar mechanism can also be assumed for these elements. Recent work by Grgur et al. [24] and Mukerjee et al. [25] on Pt–Mo alloy catalysts supports this explanation.

Nevertheless, microstructural effects caused by the addition of transition metal oxides to Pt–Ru catalysts prepared by the Adams method cannot be excluded as possible explanation for the different catalytic behavior.

4. Conclusions

The ternary catalysts prepared by a modified Adams method consist of varying amounts of noble metal oxides next to Pt–Ru alloy phases. XRD analysis indicates furthermore that the transition metal oxides exist as an amorphous structure.

The Pt–Ru particle size calculated from the Scherrer equation is 3–5 nm in diameter, which is in good agreement with calculated particle sizes from the BET surface areas of 80–120 m^2/g. Introduction of a transition metal-oxide like WO_x, MoO_x and VO_x to Pt–Ru catalysts leads to a decrease in polarization of the methanol electrodes. The ternary compound apparently influences the rate of methanol oxidation and surface oxide formation. The most prominent effect on the catalytic activity could be shown for the VO_x-containing catalyst.

Further work on ternary catalysts is in progress.

Acknowledgements

The work was partially supported by Stiftung Energieforschung Baden Württemberg under contract no. A000009696. XPS results were obtained in cooperation with the University of New South Wales UNSW, Sydney. This cooperation was sponsored by the ''DAAD Hochschulsonderprogramm III von Bund und Ländern''. The authors would like to thank Prof. R. Howe, Prof. R. Lamb, Dr. A. Hartmann, Dr. A. Buckley and S. Thompson at UNSW for their support.

References

[1] M.P. Hogarth, G.A. Hards, Platinum Met. Rev. 40 (1996) 150.
[2] T. Iwasita-Vielstich, in: H. Gerischer, C.W. Tobias (Eds.), Advances in Electrochemical Science and Engineering, 1st edn., VCH, Weinheim, 1990, p. 127.
[3] N. Marcovic, H.A. Gasteiger, P.N. Ross, X. Jiang, I. Villegas, M.J. Weaver, Electrochim. Acta 141 (1995) 91.
[4] K. Wang, H.A. Gasteiger, N.M. Marcovic, P.N. Ross Jr., Electrochim. Acta 41 (1996) 2587.
[5] E. Ticanelli, J.G. Beery, M.T. Paffet, S. Gottesfeld, J. Electroanal. Chem. 258 (1989) 61.
[6] P.K. Shen, K. Chen, A.C.C. Tseung, J. Chem. Soc. Faraday Trans. 90 (1994) 3089.
[7] K. Lasch, Untersuchungen Metalloxidhaltiger Katalysatoren für die Elektrochemische Oxidation von Methanol, ZSW, Ulm, 1996.
[8] H. Binder, A. Köhling, G. Sandstede, Energy Conversion 11 (1971) 17.
[9] M. Götz, H. Wendt, Electrochim. Acta 43 (1998) 3637.
[10] M. Götz, H. Wendt, in: S. Gottesfeld, T.F. Fuller (Eds.), Proceedings of the 2nd International Symposium on Proton Conducting Membrane Fuel Cells, Vol. 98-27, 1999, p. 291.
[11] R. Adams, R.L. Schriner, J. Am. Chem. Soc. 45 (1923) 2171.
[12] L.W. Niedrach, D.W. Mc Kee, J. Paynter, I.F. Danzig, Electrochem. Technol. 5 (1967) 318.
[13] D.A. Shirley, Phys. Rev. B 5 (1972) 4709.
[14] C.D. Wagner, L.E. Davis, R.H. Raymond, Surf. Interface Anal. 3 (1981) 211.
[15] T.J. Schmidt, M. Noeske, H.A. Gasteiger, R.J. Behm, J. Electrochem. Soc. 145 (1998) 925.
[16] M. Watanabe, H. Igarashi, K. Yosioka, Electrochim. Acta 40 (1995) 329.
[17] T.J. Schmidt, H.A. Gasteiger, G.D. Stäb, P.M. Urban, D.M. Kolb, R.J. Behm, J. Electrochem. Soc. 145 (1998) 2354.
[18] J.F. Moulder, W.F. Stickle, P.E. Sobol, K.D. Bomben, Handbook of X-Ray Photoelectron Spectroscopy, Perkin Elmer, USA, 1992.
[19] R. Kötz, H.J. Lewerenz, S. Stucki, J. Electrochem. Soc. 130 (1983) 825.
[20] B.E. Warren, X-ray Diffraction, Addison-Welsley, Reading, MA, 1996.
[21] P.K. Shen, A.C.C. Tseung, J. Electrochem. Soc. 141 (1994) 3082.
[22] A.K. Shukla, M.K. Ravikumar, A.S. Aricò, G. Candiano, V. Antonucci, N. Giordano, A. Hamnett, J. Appl. Electrochem. 25 (1995) 528.
[23] K. Machida, M. Enyo, G. Adachi, J. Shiokawa, J. Electrochem. Soc. 135 (1988) 1955.
[24] B.N. Grgur, N.M. Marcovic, P.N. Ross Jr., in: S. Gottesfeld, T.F. Fuller (Eds.), Proceedings of the 2nd International Symposium on Proton Conducting Membrane Fuel Cells, Vol. 98-27, 1999, p. 176.
[25] S. Mukerjee, S.J. Lee, E.A. Ticianelli, J. McBreen, B.N. Grgur, N.M. Marcovic, P.N. Ross Jr., J.R. Giallombardo, E.S. De Castro, Electrochem. Solid State Lett. 2 (12–15) (1999) 12.